Bitlis Eren Üniversitesi Fen Bilimleri Dergisi
BİTLİS EREN UNIVERSITY JOURNAL OF SCIENCE
ISSN: 2147-3129/e-ISSN: 2147-3188
VOLUME: 11 NO: 4 PAGE: 1084-1092 YEAR: 2022
DOI: 10.17798/bitlisfen.1174512

The Separation of glaucoma and non-glaucoma fundus images using EfficientNet-B0

Buket TOPTAŞ[1*], Davut HANBAY[2]

[1]*Computer Eng Dept., Engineering and Natural Science Faculty, Bandırma University Onyedi Eylül University Balıkesit, Turkey*
[2]*Computer Eng Dept., Engineering Faculty, Inonu University, 44280 Malatya, Turkye*
(ORCID: 0000-0003-2556-8199) (ORCID: 0000-0003-2271-7865)

EfficientNet, Glaucoma, Fundus Image

Abstract

Glaucoma is an eye disease that causes vision loss. This disease progresses silently without symptoms. Therefore, it is a difficult disease to detect. If glaucoma is detected before it progresses to advanced stages, vision loss can be prevented. Computer-aided diagnosis systems are preferred to understand whether the fundus image contains glaucoma. These systems provide accurate classification of healthy and glaucoma images. In this article, a system to separate images of a fundus dataset as glaucoma or healthy is proposed. The EfficientNet B0 model, which is a deep learning model, is used in the proposed system. The input of this deep network model is designed as six layers. The experimental results of the designed model were obtained on the publicly available ACRIMA dataset images. In the end, the average accuracy rate was determined to be 0.9775.

1. Introduction

Fundus images are frequently used in the examination of eye diseases. Ophthalmologists make a diagnosis by examining these images. However, reasons such as fatigue of the ophthalmologist, observation errors, and poor image may cause misleading results. Computer-aided diagnosis systems (CADs) are needed to reduce these misleading results. These systems are designed to assist ophthalmologists and support diagnostic accuracy. The most distinctive features of these systems are that they produce reliable, fast, and robust results.

There are many CADs proposed in the literature on glaucoma. Muramatsu et al. proposed a method that analyzes the optic disc (OD) and automatically measures the CDR ratio [1]. The method uses stereo images. These images are obtained of patients with glaucoma symptoms and healthy patients. In the proposed method, an edge detector and active contour method are used. Thus, the OD is segmented. A depth map is created to remove the unevenness of the stereo images. Noises on the depth map are reduced using mean and median filters. Next, edges are searched in radial directions on the depth maps. Thus, the optic cup (OC) contours are determined. After determining the OD and OC contours, the CDR ratio is calculated. Issac et al. presented a method of diagnosing glaucoma disease using CDR, the Neuroretinal rim (NRR), and the blood vessels in the OD region [2]. The method is based on image processing. This method is designed to be invariant to the quality of the images and resistant to noise. The OC region is segmented using the R channel of the fundus image in RGB space, and the OD region is segmented using the G channel. Then, CDR, ISNT, and NRR ratios are extracted as features. Extracted features are given to various classifiers and classification is provided. Divya et al. presented a feature-based method for the diagnosis of glaucoma [3]. Firstly, the gray-scale image of the color fundus image is obtained, and the color fundus image is divided into color channels. Then, a 2-D empirical wavelet transform is used to generate the sub-band images. Co-entropy is subtracted from the

* Corresponding author: btoptas@bandirma.edu.tr
Received:13.09.2022, Accepted: 02.11.2022

disaggregated components. Some of the obtained features are selected using student-t and principal component analysis methods. A least-squares support vector machine is used to classify features as glaucoma or non-glaucoma. Al-Bander et al. proposed a deep learning-based method to segment OD and OC regions [4]. In this method, the DenseNet network architecture is used. Fundus images are given as input to the network and trained without preprocessing. Then, preprocessed fundus images are given to the network, which it has never seen before, and segmentation of the relevant regions is performed. The CDR ratio is calculated by segmenting the OD and OC regions. The CDR ratio has been used in the diagnosis of glaucoma. Gómez-Valverde et al. conducted a study evaluating the application of different CNN architectures for glaucoma detection [5]. In the study, the success of many network architectures on fundus images with the transfer learning method was examined. All fundus images were preprocessed to train the meshes homogeneously. Optical disc were centered and the same size standard patches were used for all datasets. Also, the mean in each channel is subtracted to ensure that all data inputs have a concentric distribution. Finally, all CNN network architectures are compared and their performances are evaluated. Yu et al. performed optic disc segmentation with a customized U-net architecture for glaucoma detection [6]. The customized U-net architecture is obtained by combining the encoding layers of the trained ResNet-34 model with the classical U-net decoding layers. Pre-processed fundus images are reproduced by data augmentation methods. Then, the OD and OC regions of the images given to the model training are determined. Claro et al. proposed a method that extracts features from fundus image pixels. This method allows for the classification of retinal fundus images as glaucoma or non-glaucoma [7]. Methods such as local binary texture, gray level co-occurrence matrix, histogram of directed gradients, Tamura and gray level running length matrix, morphology, and CNN architecture are used as feature extraction methods. Extracted features were selected according to the earnings ratio. The selected features were classified by giving them to the classifiers. Through the generative adversarial network (GAN) algorithm [8], Bisneto et al. developed a method for diagnosing glaucoma disease. In the method, the training of the GAN is carried out for the segmentation of the OD region. Then, the images are subjected to the post-processing process. At this stage, the holes in the segmented OD region are filled and contrast enhancement is performed. Then, using the taxonomic diversity index, the tissue features of the OD region are extracted. The WEKA program was used as the classifier, and the results were verified here. Pruthi et al. presented the firefly swarm optimization algorithm [9]. This algorithm is designed to facilitate automatic detection of the OD region in fundus images. OC pixels are the brightest pixels in the OD region. Therefore, all the light worms have moved to the OC region, which is the brightest region. This method has been tested in various optimization algorithms. Nayak et al. used an evolutionary convolutional network to automatically detect glaucoma [10]. This network is designed for feature extraction. A real coded genetic algorithm is used to improve the weights in the layers of the network. The network architecture is trained using a criterion that maximizes the distance between classes and minimizes within-class variance. The final features were classified with many different classifiers and the success of the system was proven. Mrad et al. proposed a system that can detect glaucoma disease [11]. Fundus images captured from a smartphone are used as retinal images. The ROI region is selected from fundus images, and images are preprocessed with the CLAHE method. Blood vessels are extracted from the preprocessed ROI images. At this stage, morphological operations are used. Then, the localization of the OD region is determined. Thus, there extracted the feature from the OD region. In feature extraction, the NNR and ISNT rule (inferior (I) > superior (S) > nasal (N) > temporal (T)) are used. These features are classified by support vector machines.

As technological developments progress, CADs about glaucoma are also advancing and developing. Although many methods have been proposed and many systems have been designed in this field, it is still a field open to research. In this paper, the EfficientNet model, which has emerged in recent years and is a deep learning network model, is used. With this model, fundus images are classified as healthy and glaucoma. The performance of the proposed method has been tested on the publicly available ACRIMA dataset. Test results are presented with various performance measurement metrics.

The rest of the paper is organized as follows. Firstly, the material and method are explained. In this section, the datasets used in the proposed method, related work, and the proposed method are presented. Then, the experimental results and discussion of the proposed approach are given. In this section, the main stages of the study are explained. In addition, in this section comparisons and discussions of the experimental results with other literature studies are made. Later, the conclusions section is given. In this section, the proposed method is evaluated.

2. Material and Method

In this section, each related work is detailed in the subsequent subsections.

2.1. Dataset Used

The ACRIMA dataset is a publicly available fundus image dataset [12]. This dataset consists of glaucoma and healthy fundus images. It has 705 fundus images in total. 396 of these images are fundus images of glaucoma, and 309 of them are healthy. Image classification was done by an experienced glaucoma expert. These dataset images contain only the OD region. All images were acquired with the Topcon TRC retina camera and have a FOV of 35º. A few of the images from this data set are given in Figure 1.

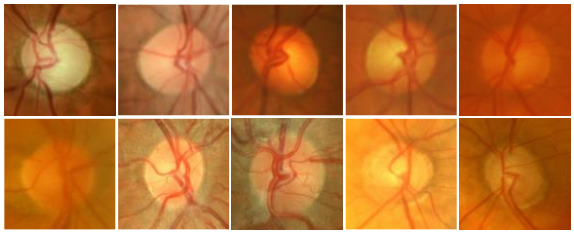

Figure 1. The first row is healthy images, the second row is images with glaucoma

2.2. Contrast Limit Adaptive Histogram Equalization

It is a method developed by Pizer et al. [13] for image enhancement. This method first splits the original image into the M×N size regions. It then calculates the gray-level histogram for each of these regions. Firstly, the average gray level pixel values are calculated for each region. The histogram of each region is then cropped according to the clipping boundary. This boundary is determined by the user. Then, the cumulative distribution function of the contrast bound histogram values is determined. Finally, each pixel value is mapped using the bi-linear interpolation method. This method has been applied to fundus images in previous studies and has produced successful results [14-17].

2.3. EfficientNet

EfficientNet is a deep learning network architecture developed in 2019 [18]. This architecture gives the relationship between three terms that significantly affect the performance of deep network architectures. These terms are depth, width, and resolution. This architecture is based on the decompound scaling method. In the first step of this method, a grid search algorithm is used. This algorithm allows the network to establish the relationship between different scaling dimensions. The target deep learning network is started with the specified scaling dimensions [19]. Mathematical expressions for the composite scaling method are given in Equations (1)-(3).

$$\alpha^{\phi}, w=\beta^{\phi}, r=\gamma^{\phi} \quad (1)$$

$$\alpha.\beta^2.\gamma^2 \approx 2 \quad (2)$$

$$\alpha \geq 1, \beta \geq 1, \gamma > 1 \quad (3)$$

where, the ϕ parameter represents a user-defined coefficient. The α, β, γ parameters are used for depth, width and resolution, respectively.
Depth is related to the number of layers of a deep learning network architecture. A deep network can get complex features by going into more detail. However, increasing the depth of the network is not always desirable because the depth will cause a cost increase and loss of time. Also, increased accuracy gain may not always be predicted. Width is related to the size of the layers of deep network architecture. The increase of neurons in the layers causes the expansion of the network. Resolution is related to the aspect ratio of the input data of a deep learning network architecture. The high resolution of the input image contains fine details in the image. Tan et al. [18] developed the EfficientNet-B0 architecture, known as the starter model. The parameter values of this architecture are given in Table 1

Table 1. EfficientNet-B0 architecture

Stage	Operator	Resolution	Channels	Layer
1	Conv 3×3	224×224	32	1
2	MBCon1, k3×3	112×112	16	1
3	MBCon6, k3×3	112×112	24	2
4	MBCon6, k5×5	56×56	40	2
5	MBCon6, k3×3	28×28	80	3
6	MBCon6, k5×5	14×14	112	3
7	MBCon6, k5×5	14×14	192	4
8	MBCon6, k3×3	7×7	320	1
9	Conv 1×1 & Pooling & FC	7×7	1280	1

2.4. Proposed Methodology

In this paper, the EfficientNet-B0 model is used to separate color fundus images of glaucoma from non-glaucoma. The flow diagram of this method is shown in Figure 2. Firstly, in this method, the input images are prepared. Then, a data augmentation technique is applied to these images. Thus, image diversity is provided and the number of images is increased. Secondly, the prepared input images are given to the EfficientNet-B0 model. As a result of the deep learning model, glaucoma and non-glaucoma fundus images are separated. The final results obtained are tested on various performance measures.

Firstly, in the proposed method, the input data of the EfficientNet-B0 model is prepared. This input data has six channels. The first channel is the first channel of the new color space proposed by [20]. This color space is created to reveal the OD region in fundus images. The OD region provides information about glaucoma disease. Therefore, this new color space is preferred in the proposed method. You can find the details of obtaining the new color space in the original article. The second channel is the R channel of the CLAHE method applied to the original fundus image. The third channel is the G channel of the CLAHE method applied to the original fundus image. These two-color channels have been used frequently in previous studies on fundus images [21],[2]. The R channel is effective in the OD region due to the intensity of the red hue. The G channel reveals the retinal vessels. The effect of this color channel is important, as there are retinal main vessels in the OD region. The last three channels are a three-channel image with a Gaussian filter applied to the new color space. Here, the core of the Gaussian filter is chosen with a size of 15×15 pixels. The Gaussian filter blurs the image by removing noise. The process of obtaining the six-channel input image is given in Figure 3.

The first block in Figure 3 is the preferred color channel. The second block is the six-channel input image obtained.

The next stage of the proposed method is the data augmentation stage. As it is known, deep learning is more successful in big data. However, datasets are limited. In this case, data augmentation is required. These operations diversify and increase the number of data. Some of these data augmentation methods are operations such as rotating, scaling, flipping, cropping, and color space transformation. In this proposed method, the rotate operation is used for the ACRIMA dataset. In this process, each fundus image is rotated at 0-9-degree angle. This data augmentation technique is the technique with the best experimental success. It has also been used in other fundus studies and has proven successful [22]. The data numbers of the ACRIMA data set after data augmentation are given in Table 2.

Table 2. The number of fundus images after data augmentation

Fundus Image	Original	Data augmentation
Glaucoma	396	3960
Non-Glaucoma	309	3090
Total	705	7050

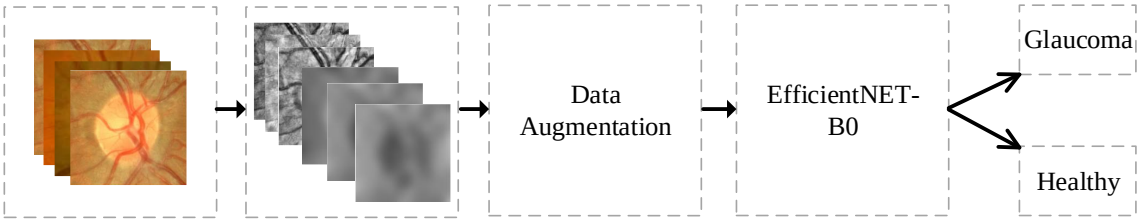

Figure 2. Flow Diagram

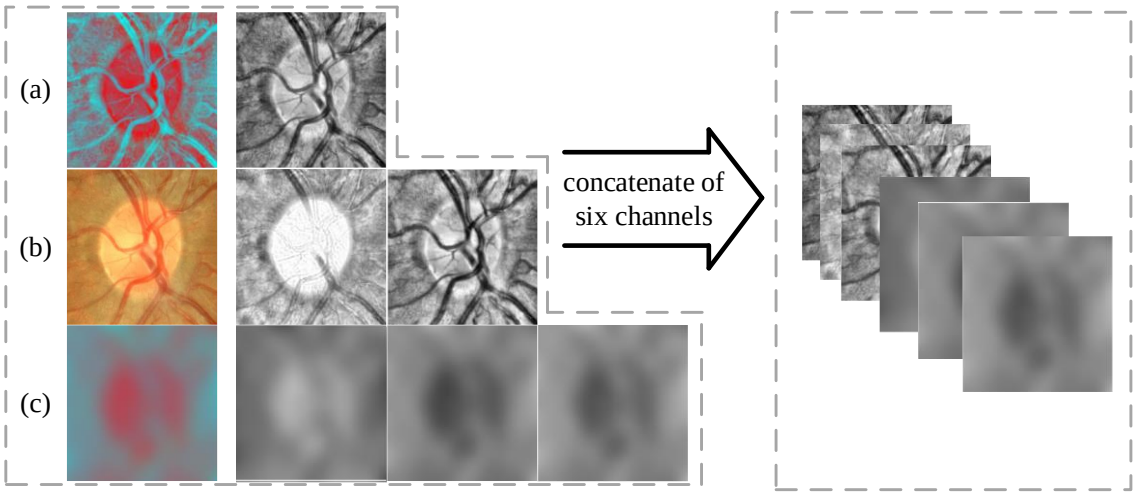

Figure 3. Six-channel input display. (a) New color space and the first channel of this color space, (b) original fundus image and R, G channel this image, (c) gaussian image result applied on (a) and color channels of this image

3. Experimental Result and Discussion

3.1. Performance Metrics

Performance metrics are used to demonstrate the experimental success of the proposed method. The most frequently used performance metrics are used to make the method comparable. The metrics used are accuracy, sensitivity, specificity, precision, and F-measure, respectively. The mathematical expressions of these metrics are given in Equations (4) -(8).

$$\text{Accuracy (Acc)}=(TP+TN)/(TP+TN+FP+FN) \quad (4)$$

$$\text{Sensitivity (Sn)/Recall}=TP/(TP+FN) \quad (5)$$

$$\text{Specificity (Sp)}=TN/(TN+FP) \quad (6)$$

$$\text{Precision (Pr)}=TP/(TP+FP) \quad (7)$$

$$\text{F-measure}=(2*\text{Precision}*\text{Recall})/(\text{Precision}+\text{Recall}) \quad (8)$$

3.2. EfficientNet-B0 Architecture

The structure of this architecture is given in Table 3. The images obtained after data augmentation are divided into three groups. The reason for this is to use different data in training, validation, and testing processes. The number of data used in training, validation, and testing processes is given in Table 3. The deep network architecture has trained and tested the ACRIMA dataset based on these data numbers.

Table 3. The number of training, validation, and test data

Fundus Image	Train	Validation	Test
Glaucoma	2440	610	910
Non-Glaucoma	1600	400	1090
Total	4040	1010	2000

There are parameters that affect the performance of the proposed method. These parameters are called hyper-parameters. The selection of hyper-parameters is very important for the model to give the best performance. Here, optimization of learning parameters is performed with stochastic gradient descent with momentum (SGDM). In this network architecture, the initial learning rate is used in two ways. Firstly, its value is set to 0.0001. This rate is kept constant throughout the network training. The training is completed with a learning rate of 0.0001 in different epoch numbers. Secondly, the initial learning rate is started from 0.001. This rate is multiplied by 0.9 in each epoch. Thus, the initial learning rate is reduced at each epoch and given to the network. The deep network architecture is shuffled in each epoch to prevent overfitting. The mini-batch parameter is for processing multiple inputs piece by piece, not altogether. In this method, the mini-batch size value is set to 32. Thus, the training of the model is done in this batch size in each iteration.

The experimental results of the proposed method are obtained by studying the learning rates mentioned above in different epochs. The learning rate is kept constant and runs for 10, 25, and 50 epochs, respectively. The accuracy metric of the results

obtained in this experimental study is 0.9235, 0.9650, and 0.9465, respectively. When the learning rate is reduced in each epoch, the accuracy of the results for 10, 25, and 50 epochs, respectively, is 0.9655, 0.9775, and 0.9750. Here, the highest accuracy rate was obtained in 25 epochs at a non-constant learning rate. Table 4 shows the results of other performance metrics at three epochs and two learning rates.

Table 4. Constant learning rate (0.0001)

Performance metrics	Maximum epoch		
	10	25	50
Accuracy	0.9235	0.9650	0.9465
Sensitivity	0.8890	0.9375	0.9118
Specificity	0.9562	0.9904	0.9795
Precision	0.9505	0.9890	0.9769
F-measure	0.9187	0.9626	0.9432
Training Time (s)	1551	3949	8054

Table 5. Reduced learning rate (each epoch)

Performance metrics	Maximum epoch		
	10	25	50
Accuracy	0.9655	**0.9775**	0.9750
Sensitivity	0.9394	**0.9577**	0.9498
Specificity	0.9895	0.9953	**0.9981**
Precision	0.9879	0.9945	**0.9978**
F-measure	0.9630	**0.9757**	0.9732
Training Time (s)	1562	3829	**7613**

In Table 5, the highest performance metric values are given in bold. Considering the performance metric results obtained in Table 4 and Table 5, the highest result was obtained with the decreasing learning rate in each epoch. It can be said that the ideal epoch number is between 25 and50. As a result of the accuracy being taken at 50 epochs, there was a decrease of 0.0025. However, Sp and Pr parameters increased. The confusion matrix of the EfficientNet-B0 architecture trained according to these hyper parameters is given in Figure 4. In this matrix, the intersection of 'true healthy' and 'predicted healthy' is represented by the parameter TN. The intersection of 'true healthy' and 'predicted glaucoma' is represented by the FN parameter. The intersection of 'true glaucoma' and 'predicted healthy' is represented by the FP parameter. The intersection of 'true glaucoma' and 'predicted glaucoma' is represented by the TP parameter.

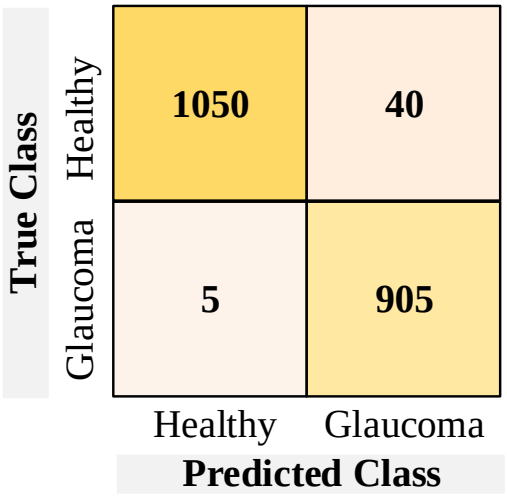

Figure 4. Confusion Matrix

The proposed method was compared with the state-of-the-art technological methods according to the performance metric parameters. This comparison process is given in Table 6.

According to this table, the proposed method showed a competitive performance. The results obtained are quantitative proof that the proposed method is the correct method. Ultimately, it has been shown that the EfficientNet-B0 model can differentiate fundus photographs from glaucoma and healthy in clinical settings.

4. The Conclusions

The proposed method aims to classify a fundus image as glaucoma or healthy without human intervention. The performance metrics of the proposed method showed better performance compared to the state-of-the-art methods. These performance metrics reflect the effectiveness of the EfficientNet-B0 model for glaucoma disease.

The performance results of the proposed method are obtained from the publicly available ACRIMA dataset. The hyper-parameters of the EfficientNet-B0 model are set as mentioned in Section 3.2. Here, the learning rate of the model is initialized at 0.001 and decreased at each epoch. The epoch number was determined as 25. Firstly, the original dataset images are given to this tuned model. Here, the performance metrics of the obtained results were calculated as 0.9610 for the Acc metric, 0.9315 for the Sp metric, 0.9884 for the Sn metric, 0.9868 for the Pr metric, and 0.9584 for the F-measure metric. In this experiment, it was observed that the details of the image were lost in the hierarchy of the network. Therefore, to reliably distinguish images with glaucoma, the input images are set to have six layers. Then, data augmentation was applied so that the input images are diverse and prevent overfitting. Thus, the performance metrics of the results obtained were calculated as 0. 9775 for the Acc metric, 0.9577 for the Sp metric, 0.9953 for the Sn metric, 0.9945 for the Pr metric, and 0.9757 for the F-measure metric. Considering these metrics parameters, the positive effects of the proposed six-layer input image are clearly evident. The scope of the proposed method is to present a useful CAD system that can distinguish between glaucoma and healthy images on retinal fundus images. In this method, glaucoma disease was used in the new color space for the first time. The aim in the future is to use the EfficienNet-B0 model and other EfficientNet models in different datasets on glaucoma disease.

Table 6. Other state-of-the-art methods that separate glaucoma and healthy fundus images using the ACRIMA dataset

Author	Method(s)	Data augmentation	Performance measures
[22]	CNN	Applied (G:3960 Non-G:3090)	Acc:0.9664 Sn:0.9607 Sp:0.9739 Pr:0.977
[23]	ResNet-152	Applied (G:2976 Non-G: 2400)	Auc:0.77 Acc:0.48 Sp: 0.83
[24]	UCSD and UTokyo	Not Applied	Auc:0.86
[25]	CDR and using traditional method	Not Applied	Acc:0.9461 Sp:0.9500 Se:0.9457
Proposed Method	EfficientNet-B0	Applied (G:3960 Non-G:3090)	Acc:0.9775 Se: 0.9577 Pr:0.9945 Sp:0.9953

F1-measure: 0.9757

Contributions of the Authors

In the scope of this study, Author 1 put forward the formation of idea, performed the design and the spelling, and checked the article; Author 2 is examined the results for the article in terms of content were contributed.

Conflict of Interest Statement

There is no conflict of interest between the authors.

Statement of Research and Publication Ethics

There is no need to obtain permission from the ethics committee for the article prepared. There is no conflict of interest with any person / institution in the article prepared.

References

[1] Muramatsu C, Nakagawa T, Sawada A, Hatanaka Y, Yamamoto T, Fujita H. "*Automated determination of cup-to-disc ratio for classification of glaucomatous and normal eyes on stereo retinal fundus images*". J Biomed Opt., 16(9), 2011.

[2] Issac A, Partha SM, Dutta MK. "*An adaptive threshold-based image processing technique for improved glaucoma detection and classification*". Computer Methods and Programs in Biomedicine, 122(2):229–244, 2015

[3] Divya L, Jacob J. "*Performance analysis of glaucoma detection approaches from fundus images*". Procedia Computer Science, 143:544–551. 8th International Conference on Advances in Computing and Communications (ICACC-2018)

[4] Al-Bander B, Williams BM, Al-Nuaimy W, Al-Taee MA, Pratt H, Zheng Y. "*Dense fully convolutional segmentation of the optic disc and cup in colour fundus for glaucoma diagnosis*". Symmetry, 10(4),2018.

[5] Gómez-Valverde JJ, Antón A, Fatti G, Liefers B, Herranz A, Santos A, ... Ledesma-CMJ. "*Automatic glaucoma classification using color fundus images based on convolutional neural networks and transfer learning*". Biomedical optics express, 10(2), 892-913,2019.

[6] Yu S, Xiao D, Frost S, Kanagasingam Y. "*Robust optic disc and cup segmentation with deep learning for glaucoma detection*". Computerized Medical Imaging and Graphics, 74:61–71,2019

[7] Claro M, Veras R, Santana A, Araujo F, Silva R, Almeida, J, Leite D. "*An hybrid feature space from texture information and transfer learning for glaucoma classification*". Journal of Visual Communication and Image Representation, 64:102597,2019.

[8] Bisneto TRV, de Carvalho FAO, Magalhaes DMV. "*Generative Adversarial network and texture features applied to automatic glaucoma detection*". Appl. Soft Comput., 90:106165,2020

[9] Pruthi J, Khanna K, Arora S. "*Optic cup segmentation from retinal fundus images using glowworm swarm optimization for glaucoma detection*". Biomedical Signal Processing and Control, 60:102004, 2020.

[10] Nayak DR, Das D, Majhi B, Bhandary SV, Acharya UR. "*Ecnet: An evolutionary convolutional network for automated glaucoma detection using fundus images*". Biomedical Signal Processing and Control, 67:102559, 2021.

[11] Mrad Y, Elloumi Y, Akil M, Bedoui M. "*A fast and accurate method for glaucoma screening from smartphone-captured fundus images*". IRBM,2021.

[12] Diaz-Pinto A, Morales S, Naranjo V, Kohler T, Mossi JM, Navea A. (2019). "*Cnns for automatic glaucoma assessment using fundus images: an extensive validation*". BioMed Eng OnLine,18(29), 2019.

[13] Pizer SM, Amburn EP, Austin JD, Cromartie R, Geselowitz A, Greer T, ter Haar RB, Zimmerman JB, Zuiderveld K. "*Adaptive histogram equalization and its variations*". Computer Vision, Graphics, and Image Processing, 39(3):355–368, 1987.

[14] dos Santos JCM, Carrijo GA, de Fátima dos SCC., Ferreira JC, Sousa PM, Patrocínio AC. "*Fundus image quality enhancement for blood vessel detection via a neural network using CLAHE and Wiener filter*". Research on Biomedical Engineering, 36(2), 107-119, 2020.

[15] Sonali SS, Singh AK, Ghrera S, Elhoseny M. "*An approach for de-noising and contrast enhancement of retinal fundus image using clahe*". Optics and Laser Technology, 110:87–98, 2019.
[16] Toptaş B, Hanbay D. "*Retinal blood vessel segmentation using pixel-based feature vector*". Biomedical Signal Processing and Control, 70:103053, 2021.
[17] Uysal E, Güraksin G. "*Computer-aided retinal vessel segmentation in retinal images: convolutional neural networks*". Multimed Tools Appl, 80, 2021.
[18] Tan M, Le Q. "*Efficientnet: Rethinking model scaling for convolutional neural networks*". In International conference on machine learning (pp. 6105-6114). PMLR.,2019.
[19] Gupta N, Garg H, Agarwal R. "*A robust framework for glaucoma detection using CLAHE and EfficientNet*". The Visual Computer, 1-14,2021.
[20] Toptaş B, Toptaş M, Hanbay D. "*Detection of Optic Disc Localization from Retinal Fundus Image Using Optimized Color Space*". Journal of Digital Imaging, 1-18,2022.
[21] Azzopardi G, Strisciuglio N, Vento M, Petkov N. "*Trainable COSFIRE filters for vessel delineation with application to retinal images*". Medical image analysis, 19(1), 46-57,2015.
[22] Elangovan P, Nath MK. "*Glaucoma assessment from color fundus images using convolutional neural network*" International Journal of Imaging Systems and Technology, 31(2), 955-971,2021.
[23] Serte S., Serener A. "*A generalized deep learning model for glaucoma detection*". In 2019 3rd International symposium on multidisciplinary studies and innovative technologies (ISMSIT) (pp. 1-5). IEEE,2019.
[24] Christopher M., Nakahara K., Bowd C., Proudfoot J. A., Belghith A., Goldbaum M. H., ... Zangwill L. M. "*Effects of study population, labeling and training on glaucoma detection using deep learning algorithms*". Translational vision science & technology, 9(2), 27-27,2020.
[25] Almeida-Galárraga D, Benavides-MK., Insuasti-Cruz E, Lovato-Villacís N, Suárez-Jaramillo V, Tene-Hurtado D, Tirado-Espín A, Villalba-Meneses GF. "*Glaucoma detection through digital processing from fundus images using MATLAB*". In 2021 Second International Conference on Information Systems and Software Technologies (ICI2ST) (pp. 39-45). IEEE, 2021.